Knockdown of FOXO4 protects against OGD/R-induced cerebral microvascular endothelial cell injury and regulates the AMPK/Nrf2/HO-1 pathway through transcriptional activation of CTRP6

XIANGTING CUI[1,2], ZHILI LI[1] and YUHUA YUAN[1]

[1]Clinical Laboratory, Tianjin Medical University General Hospital, Tianjin 300052; [2]Clinical Laboratory, Binhai Hospital of Tianjin Medical University General Hospital, Tianjin 300480, P.R. China

Received August 23, 2023; Accepted November 29, 2023

DOI: 10.3892/etm.2024.12382

Abstract. Cerebral ischemia is a type of cerebrovascular disease with high disability and mortality rates. The expression of forkhead box protein O4 (FOXO4) in the brain is increased following traumatic brain injury. To the best of our knowledge, however, the role of FOXO4 as well as its mechanism in cerebral ischemia has not been reported so far. For the establishment of an *in vitro* cellular injury model, human brain microvascular endothelial HCMEC/D3 cells were induced by oxygen-glucose deprivation/reoxygenation (OGD/R). mRNA and protein expressions of FOXO4 and C1q/tumor necrosis factor-related protein 6 (CTRP6) in OGD/R-induced HCMEC/D3 cells were detected by reverse transcription-quantitative (RT-q)PCR and western blotting. The transfection efficacy of small interfering (si)- and overexpression (Ov)-FOXO4 and si-CTRP6 was assessed using RT-qPCR and western blotting. Cell Counting Kit-8 and TUNEL assay were used to assess viability and apoptosis of HCMEC/D3 cells induced by OGD/R, respectively. A FITC-Dextran assay kit was applied to determine endothelial permeability and immunofluorescence assay was used for the measurement of the tight junction protein zonula occludens-1. The levels of oxidative stress markers and inflammatory cytokines were assessed with corresponding assay kits. The binding sites of transcription factor, FOXO4 and CTRP6 promoter were predicted using HDOCK SERVER. Luciferase reporter assay was used to detect the activity of the CTRP6 promoter while chromatin immunoprecipitation assay was used to evaluate the binding ability of the FOXO4 and CTRP6 promoter. Western blotting was used for the detection of apoptosis- and AMPK/Nrf2/heme oxygenase-1 (HO-1) pathway-associated proteins, along with tight junction proteins. The expression of FOXO4 was increased in OGD/R-induced HCMEC/D3 cells. After interfering with FOXO4 in cells, the viability of the OGD/R-induced HCMEC/D3 cells was increased while apoptosis was decreased. Furthermore, FOXO4 interference improved cellular barrier dysfunction but inhibited oxidative stress and the inflammatory response in HCMEC/D3 cells induced by OGD/R. FOXO4 knockdown regulated CTRP6 transcription in HCMEC/D3 cells. Knockdown of FOXO4 regulated expression of CTRP6 and protected OGD/R-induced HCMEC/D3 cell injury via the AMPK/Nrf2/HO-1 pathway. The present study indicated that FOXO4 knockdown activated CTRP6 to protect against cerebral microvascular endothelial cell injury induced by OGD/R via the AMPK/Nrf2/HO-1 pathway.

Correspondence to: Dr Yuhua Yuan, Clinical Laboratory, Tianjin Medical University General Hospital, 154 Anshan Road, Heping, Tianjin 300052, P.R. China
E-mail: yuanyuh840917@163.com

Key words: cerebral ischemia, forkhead box protein O4, C1q/tumor necrosis factor-related protein 6, AMPK/Nrf2/heme oxygenase-1 pathway, oxygen glucose deprivation/reoxygenation, microvascular endothelial cell

Introduction

In 2019, there were 12 million cases of strokes and 6.55 million stroke-related deaths worldwide, with ischemic stroke (IS) accounting for 62.4% of all stroke events, jeopardizing the health and lives of patients (1). IS constitutes the majority of stroke cases (2) and is primarily caused by cerebral ischemia and hypoxia due to decreased cerebral blood flow or insufficient oxygen supply to brain tissue. At present, the most effective clinical treatment for cerebral ischemia is to re-establish effective blood supply and restore cerebral perfusion in the ischemic area by mechanical thrombectomy and intravenous thrombolysis with drugs such as anticoagulants and, antiplatelet and thrombolytic drugs (3). However, inflammation and oxidative stress during reperfusion can cause secondary injury to brain tissue, resulting in brain dysfunction (4). This pathophysiological process is known as cerebral ischemia/reperfusion injury (CIRI).

A previous study has shown that inhibition of bromodomain-containing 4 can alleviate apoptosis and endoplasmic reperfusion injury induced by renal IRI by blocking forkhead box protein O4 (FOXO4)-mediated oxidative stress (5). FOXO4, a member of the FOXO family, is involved in numerous biological behaviors including cell energy metabolism

regulation, cell proliferation, differentiation, apoptosis, cell senescence, homeostasis and oxidative stress (6,7). However, it is unclear whether FOXO4 serves a regulatory role in CIRI. A literature review showed that protein levels of FOXO1, FOXO3a and FOXO4 are significantly increased in the brain following traumatic brain injury (8). In addition, sevoflurane has been shown to alleviate liver IRI by promoting expression of microRNA-96 and inhibiting expression of FOXO4 (9). Moreover, hypoxia/reoxygenation (H/R) induces FOXO4 upregulation in rat H9C2 cardiomyocytes, and FOXO4 overexpression can reverse the protective effects of ubiquitin-specific peptidase 10 (USP10) overexpression on H/R-induced H9C2 cells by regulating the Hippo/yes-associated protein 1 signaling pathway (10). To the best of our knowledge, however, the role of FOXO4 in cerebral ischemia has not been reported.

In the present study, the role of FOXO4 in cerebral microvascular endothelial cell injury in cerebral ischemia was investigated and its regulatory mechanisms were explored. The present study aimed to provide a theoretical basis for clinical treatment of cerebral ischemia with FOXO4.

Materials and methods

Database. HDOCK SERVER (hdock.phys.hust.edu.cn/) database (11) and JASPAR database (https://jaspar.elixir.no/) were used to predict the binding between FOXO4 and the CTRP6 promoter.

Cell culture. The human brain microvascular endothelial cell (BMEC) line HCMEC/D3 (cat. no. BNCC337728; BeNa Culture Collection) was cultured in standard DMEM with 10% FBS (both Gibco; Thermo Fisher Scientific, Inc.) at 37˚C with 5% CO_2.

Induction of the oxygen-glucose deprivation/reoxygenation (OGD/R) model. HCMEC/D3 cells were incubated in glucose-free Dulbecco's modified Eagle's medium (DMEM; Gibco; Thermo Fisher Scientific, Inc.) in a hypoxic incubator (5% CO_2, 95% N_2) at 37˚C for 2 h. Cells were removed from the anoxic atmosphere and transferred to a normal environment for 12 h. The cells cultured in serum-free medium at 37˚C with 5% CO_2 were defined as the control group.

Cell transfection. siRNAs specific to FOXO4 (si-FOXO4#1 and si-FOXO4#2) or CTRP6 (si-CTRP6#1 and si-CTRP6#2), corresponding negative control (si-NC), pc-DNA3.1 vectors containing the complete sequence of FOXO4 [overexpression (Ov-)FOXO4] and empty vector (Ov-NC) were synthesized by Shanghai GenePharma Co., Ltd. The sequences of si-FOXO4 and si-CTRP6 were as follows: si-FOXO4#1, 5'-CCGTAC TGTACCCTACTTCAAGG-3'; si-FOXO4#2, 5'-AGGATC TAGATCTTGATATGTAT-3'; si-CTRP6#1, 5'-CAACGACTT CGACACCTACAT-3'; si-CTRP6#2, 5'-GAAAGAGGCTGT CATCCTGTA-3' and si-NC, 5'-UUCUCCGAACGUGUC ACGUTT-3'. Using Lipofectamine® 3000 reagent (Invitrogen; Thermo Fisher Scientific, Inc.), 100 nM recombinants were transfected into HCMEC/D3 cells for 48 h at 37˚C. The transfection efficacy was examined with western blotting and RT-qPCR and OGD/R induction was performed 48 h after transfection.

Reverse transcription-quantitative (RT-q)PCR. RT-qPCR was applied to assess the transfection efficiency of small interfering RNAs 48 h post-transfection. Total RNA was isolated from cells using Trizol® reagent (Invitrogen; Thermo Fisher Scientific, Inc.) in accordance with the manufacturer's protocol. A total of 500 ng total RNA was used as a template to synthesize cDNA using iScript Reverse Transcription Supermix (Bio-Rad Laboratories, Inc.) according to the manufacturer's protocol. SYBR-based qPCR was performed to detect the total mRNA transcripts of the target genes on an ABI 7500 platform (Applied Biosystems; Thermo Fisher Scientific, Inc.). The relative expression of target genes was assessed using the $2^{-\Delta\Delta Cq}$ method and normalized to the housekeeping gene GAPDH (12). The following primers were used: FOXO4 forward, 5'-GGCTGCCGCGATCATAGAC-3' and reverse, 5'-GGCTGGTTAGCGATCTCTGG-3'; C1q/tumor necrosis factor-related protein 6 (CTRP6) forward, 5'-TGC CTGAGATCAGACCCTACA-3' and reverse, 5'-GCCCAC TGAGAAGGCGAAG-3' and GAPDH forward, 5'-AATGGG CAGCCGTTAGGAAA-3' and reverse, 5'-GCGCCCAAT ACGACCAAATC-3'.

Western blotting. Cell lysates were collected using RIPA (Beijing Solarbio Science & Technology Co., Ltd.). The protein concentration of cell lysates were measured with a BCA Protein Assay Kit (Sangon Biotech Co., Ltd.). Equal protein samples (30 μg per lane) were separated by 10% SDS-PAGE and transferred to PVDF membrane. The membranes, blocked using 5% BSA (Beijing Solarbio Science & Technology Co., Ltd.) for 1 h at room temperature, were incubated with primary antibodies including FOXO4 (1:1,000; cat. no. ab128908), Bcl-2 (1:2,000; cat. no. ab182858), Bax (1:1,000; cat. no. ab32503), cleaved caspase 3 (1:500; cat. no. ab32042), caspase 3 (1:5,000; cat. no. ab32351), ZO-1 (1:1,000; cat. no. ab276131), Occludin (1:1,000; cat. no. ab216327), Claudin-5 (1:1,000; cat. no. ab131259), CTRP6 (1:1,000; cat. no. ab300583) and β-actin (1:1,000; cat. no. ab8227), all from Abcam, overnight at 4˚C and then incubated with goat anti-rabbit horseradish peroxidase-conjugated IgG (1:2,000; cat. no. ab6721; Abcam) for 2 h at room temperature. Protein bands were visualized using ECL Prime Western Blotting Detection Reagent (Amersham; Cytiva) and the density of the bands was determined using ImageJ software (version 1.8.0; National Institutes of Health).

Cell viability. Cell viability was detected using a Cell Counting Kit-8 (CCK-8) assay. HCMEC/D3 cells were cultured in a 96-well plate for 24 h at 37˚C. Then, 10 μl CCK-8 solution (Dojindo Laboratories, Inc.) was added to each well and cells were incubated for 2 h. Absorbance was detected at 490 nm with a microplate reader (Bio-Rad Laboratories, Inc.).

TUNEL assay. To determine apoptosis of HCMEC/D3 cells, a TUNEL assay with an *In Situ* Cell Death Detection kit, POD (Roche Diagnostics GmbH) was performed. Apoptotic cells were fixed with 4% formaldehyde for 25 min at 4˚C and then permeabilized by 0.2% TritonX-100 for 5 min at 4˚C. The cells were equilibrated with 100 μl equilibration buffer for 10 min at room temperature. Cells were labeled with 50 μl TdT reaction mix at 37˚C for 1 h. Saline-sodium citrate (SSC) buffer was used to stop the reaction and cell nuclei were mounted

with mounting medium containing 1 mg/ml DAPI for 5 min at room temperature. The images in five random fields were obtained by fluorescence microscopy (magnification, x100).

Endothelial permeability. FITC-Dextran assay kit (cat. no. ECM644; MilliporeSigma) was used to determine endothelial permeability in accordance with the manufacturer's instructions. HCMEC/D3 cells were seeded into a Transwell chamber ($1x10^4$ cells/well; 8-μm pore size; Costar; Corning, Inc.) for 72 h at 37˚C. Then, the DMEM (Gibco; Thermo Fisher Scientific, Inc.) was discarded and cells in the upper chamber were incubated with 10 kDa FITC-dextran (10 mg/ml; 10 μl) for 1 h at 37˚C, and 50 μl of DMEM was added to the lower compartment. The plates were incubated in the dark for 60 min at 37˚C, after which the fluorescence intensity in the upper chamber was determined with a fluorescence microscope (magnification, x200) and was measured using ImageJ software (version 1.8.0; National Institutes of Health).

Immunofluorescence (IF) staining. HCMEC/D3 cells were fixed with 4% formaldehyde for 15 min at room temperature and subsequently penetrated with 0.5% Triton X-100 (Sangon Biotech Co., Ltd.) at room temperature for 20 min. Following blocking with 5% normal goat serum (Beijing Solarbio Science & Technology Co., Ltd.) for 1 h at room temperature, HCMEC/D3 cells were incubated with primary antibodies against zonula occludens-1 (ZO-1; cat. no. ab221547; 1:100; Abcam) overnight at 4˚C. The Alexa Fluor® 488-conjugated goat anti-rabbit IgG secondary antibodies (cat. no. ab150077; 1:400; Abcam) were then added to the slides at 37˚C for 1 h. Cells were incubated with DAPI for 5 min at room temperature in the dark. The cell slides were finally analyzed under a fluorescent microscope (magnification, x200; Olympus Corporation). Integrated optical density or positive cell numbers in each image were assessed using ImageJ software (version 1.8.0; National Institutes of Health).

ELISA. The levels of IL-1β, IL-10 and tumor necrosis factor-α (TNF-α) in the supernatants of HCMEC/D3 cells were examined using commercial IL-1β (cat. no. H002-1-2), IL-10 (cat. no. H009-1-2) and TNF-α (cat. no. H052-1-2) ELISA kits (all from Nanjing Jiancheng Bioengineering Institute) according to the manufacturer's instructions. Absorbance was detected at 450 nm. Cellular reactive oxygen species (ROS) assay (cat. no. E004-1-1), superoxide dismutase (SOD) activity assay (cat. no. A001-2-2) and glutathione peroxidase (GSH-Px) assay kits (cat. no. A005-1-2) all from Nanjing Jiancheng Bioengineering Institute were used to determine ROS, SOD and GSH-Px activity, respectively, according to the manufacturer's instructions.

Luciferase reporter assay. The CTRP6 promoter reporter vector [CTRP6-mutant (MUT) or wild-type (WT)] was designed and synthesized by Sangon Biotech Co., Ltd. The reporter construct was transiently transfected along with a *Renilla* control plasmid and either Ov-FOXO4 or Ov-NC using Lipofectamine® 3000 reagent (Invitrogen; Thermo Fisher Scientific, Inc.) according to the manufacturer's instructions. Following transfection for 6 h at 37˚C, the DMEM (Gibco; Thermo Fisher Scientific, Inc.) was replaced with DMEM/F12 (Gibco; Thermo Fisher Scientific, Inc.) supplemented with 0.2% FBS (Gibco; Thermo Fisher Scientific, Inc.). At 48 h post-transfection, the luciferase activity was detected using a dual-luciferase reporter assay system (Promega Corporation) and normalized to Renilla luciferase activities.

Chromatin immunoprecipitation (ChIP) assay. HCMEC/D3 cells were sonicated at 150 Hz and sheared with four sets of 10 sec pulses on wet ice to generate 200-500 bp DNA fragments. The lysate (100 μl) was immunoprecipitated with anti-FOXO4 (1:100; cat. no. ab128908; Abcam) or IgG antibodies (negative control; 1:100; cat. no. ab205718; Abcam) overnight at 4˚C. Immunoprecipitated DNAs were obtained by phenol/chloroform extraction and analyzed by RT-qPCR according to the aforementioned protocol.

Statistical analysis. All data were analyzed with GraphPad Prism 6.0 (Dotmatics) and are presented as the mean ± SD. All experiments were performed in triplicate. One-way analysis of variance followed by Tukey's post hoc test was used to assess the differences and $P<0.05$ was considered to indicate a statistically significant difference.

Results

Knockdown of FOXO4 enhances OGD/R-induced HCMEC/D3 cell viability. Following OGD/R induction, the expression of FOXO4 was detected by RT-qPCR and western blotting. mRNA and protein expressions of FOXO4 were significantly increased in HCMEC/D3 cells induced by OGD/R (Fig. 1A and B). FOXO4 interference plasmid was constructed and RT-qPCR and western blotting showed successful cell transfection (Fig. 1C and D). si-FOXO4#1 was selected for follow-up experiments because it exhibited the highest interference efficacy. CCK-8 assay showed that the cell viability of OGD/R group was significantly decreased compared with the control group. Compared with the OGD/R + si-NC group, viability of the OGD/R + si-FOXO4 group was significantly increased (Fig. 1E). Apoptosis was detected by TUNEL assay; cell apoptosis was significantly increased after OGD/R induction compared with the control group and significantly inhibited by FOXO4 interference (Fig. 2A). Western blotting of apoptosis-associated proteins showed that after OGD/R induction, the expression of Bcl-2 was significantly decreased, while expression of Bax and cleaved caspase 3 was significantly increased. These effects were all significantly reversed by si-FOXO4 in comparison with the OGD/R + si-NC group (Fig. 2B).

Knockdown of FOXO4 improves OGD/R-induced HCMEC/D3 cell barrier dysfunction. The effect of FOXO4 on cellular barrier dysfunction was examined. FITC-Dextran kit was used to detect endothelial permeability; endothelial permeability was significantly increased after OGD/R induction. Compared with the OGD/R + si-NC group, FOXO4 depletion significantly decreased endothelial permeability (Fig. 3A). IF assay detected the expression of tight junction protein ZO-1; expression of ZO-1 was decreased after OGD/R induction, while FOXO4 interference increased the expression of ZO-1 in the OGD/R + si-FOXO4 group (Fig. 3B). Western blotting detected the expression of tight junction proteins ZO-1, occludin and claudin-5;

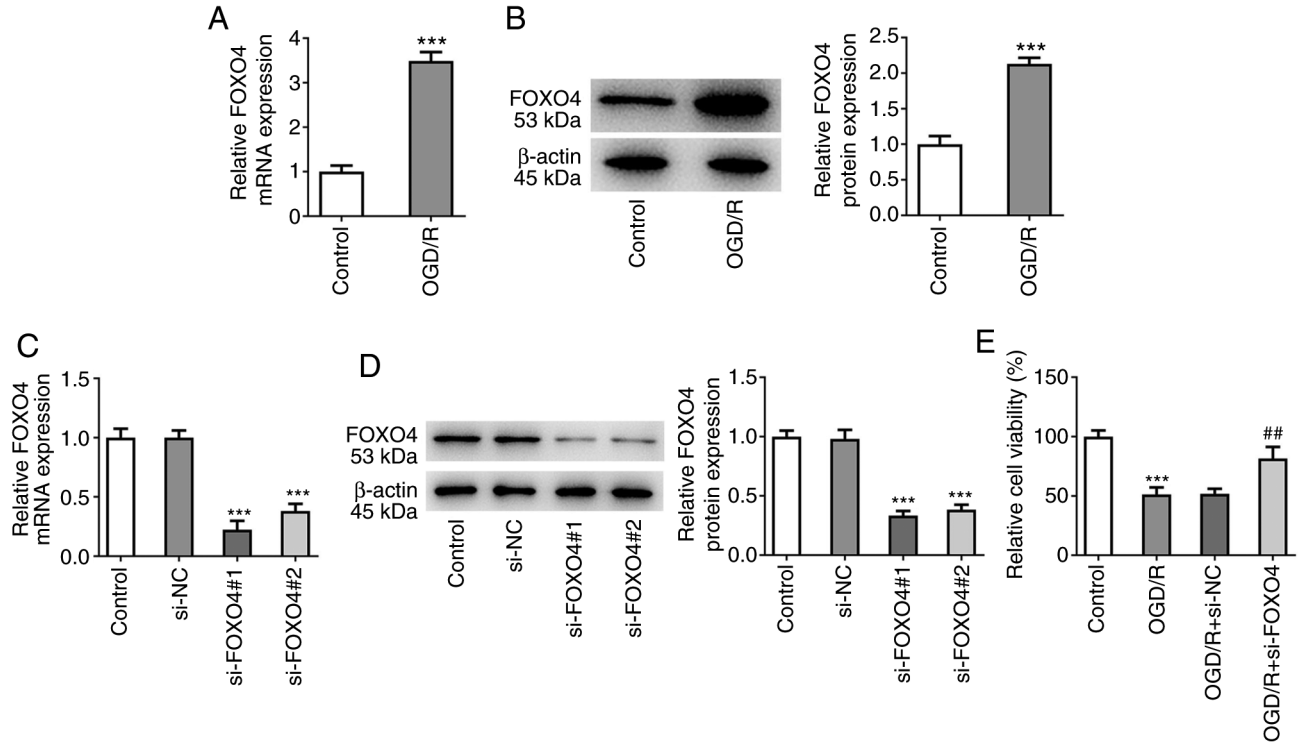

Figure 1. Knockdown of FOXO4 enhances OGD/R-induced HCMEC/D3 cell viability. Expression of FOXO4 was detected by (A) RT-qPCR and (B) western blotting. ***P<0.001 vs. control. FOXO4 interference plasmid was transfected. (C) RT-qPCR and (D) western blotting were used to detect transfection efficiency. ***P<0.001 vs. si-NC. (E) Cell Counting Kit-8 was used to detect cell viability. ***P<0.001 vs. control; ##P<0.01 vs. OGD/R + si-NC. OGD/R, oxygen-glucose deprivation/reoxygenation; FOXO4, forkhead box protein O4; NC, negative control; si, small interfering; RT-q, reverse transcription-quantitative.

compared with the control group, the expression of ZO-1, occludin and claudin-5 was decreased significantly following OGD/R induction. Compared with the OGD/R + si-NC group, the expression of ZO-1, occludin and claudin-5 was significantly increased in the OGD/R + si-FOXO4 group (Fig. 3C).

Knockdown of FOXO4 alleviates OGD/R-induced oxidative stress and inflammation in HCMEC/D3 cells. Levels of cellular oxidative stress and inflammation were measured. After OGD/R induction, the activities of SOD and GSH-Px in HCMEC/D3 cells were significantly decreased, while the activity of ROS increased. Compared with the OGD/R + si-NC group, the activities of SOD and GSH-Px in the OGD/R + si-FOXO4 group were significantly increased, while activity of ROS was decreased (Fig. 4A). ELISA was used to detect levels of inflammatory cytokines; levels of IL-6, IL-1β and TNF-α were significantly increased after OGD/R induction. Interference with FOXO4 significantly reversed the increase in IL-6, IL-1β and TNF-α (Fig. 4B). These results suggested that knockdown of FOXO4 alleviated OGD/R-induced oxidative stress and inflammation in HCMEC/D3 cells.

Knockdown of FOXO4 regulates CTRP6 transcription in HCMEC/D3 cells. The HDOCK SERVER database showed the binding of FOXO4 to CTRP6 with a -257.66 docking score and 0.8960 confidence score (Fig. 5A). Potential binding sequences between FOXO4 and CTRP6 promoter were also predicted using the JASPAR database (Fig. 5B). Moreover, mRNA and protein expression of CTRP6 was significantly decreased in OGD/R-induced HCMEC/D3 cells (Fig. 5C and D). FOXO4 was overexpressed in HCMEC/D3 cells and its transfection efficiency was assessed (Fig. 5E and F). RT-qPCR and western blotting results showed that the mRNA and protein expression of CTRP6 in Ov-FOXO4 group was significantly decreased compared with the Ov-NC group. Following interference with FOXO4, CTRP6 expression in si-FOXO4 group was significantly increased compared with the si-NC group (Fig. 5G and H). Moreover, luciferase detection and ChIP assay both demonstrated the binding ability of FOXO4 and CTRP6 promoter (Fig. 5I and J). These results indicated that FOXO4 inhibited expression of CTRP6.

Knockdown of FOXO4 regulates expression of CTRP6 to protect against OGD/R-induced HCMEC/D3 cell damage. CTRP6 interference plasmid was constructed and si-CTRP6#2 was selected for subsequent experiments due to its strong interference efficiency (Fig. 6A and B). TUNEL assay and western blotting showed that, compared with the OGD/R + si-FOXO4 + si-NC group, cell apoptosis in OGD/R + si-FOXO4 + si-CTRP6 group was significantly increased, accompanied by decreased expression of Bcl-2 and increased expression of Bax and cleaved caspase 3 (Fig. 6C and D). FITC-Dextran assay results showed that interference with CTRP6 significantly reversed the inhibitory effect of FOXO4 interference on OGD/R-induced endothelial permeability (Fig. 7A). IF assay showed that compared with the OGD/R + si-FOXO4 + si-NC group, expression of ZO-1 in the OGD/R + si-FOXO4 + si-CTRP6 group was significantly decreased (Fig. 7B). Moreover, western blotting showed that compared with the OGD/R + si-FOXO4 +

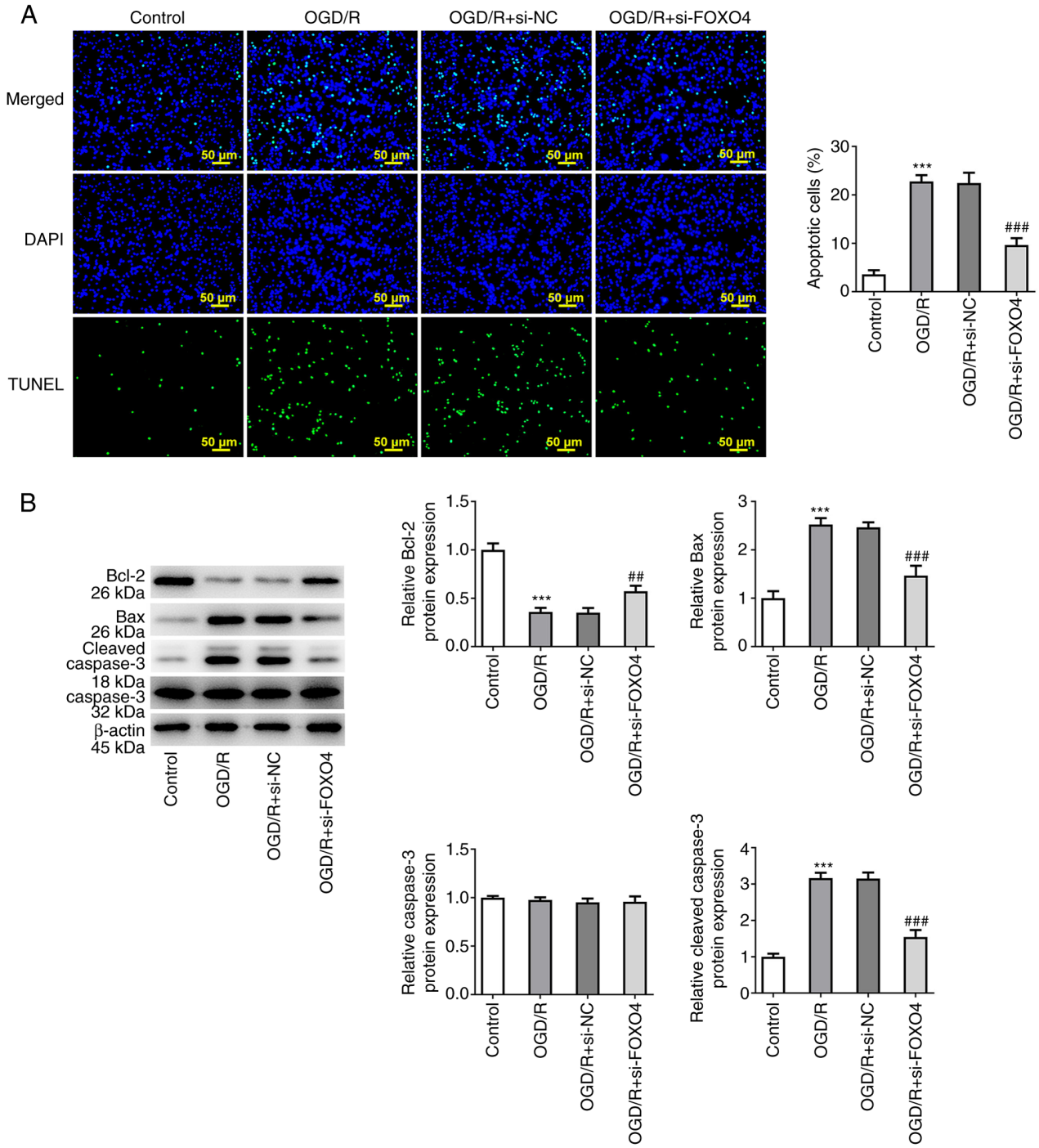

Figure 2. Knockdown of FOXO4 promotes OGD/R-induced HCMEC/D3 cell apoptosis. (A) Apoptosis was detected by TUNEL assay. (B) Western blotting detected expression of apoptosis-associated proteins. ***P<0.001 vs. control; ##P<0.01, ###P<0.001 vs. OGD/R + si-NC. OGD/R, oxygen-glucose deprivation/reoxygenation; FOXO4, forkhead box protein O4; NC, negative control; si, small interfering.

si-NC group, expression of ZO-1, occludin and claudin-5 in the OGD/R + si-FOXO4 + si-CTRP6 group was significantly decreased (Fig. 7C). In addition, compared with the OGD/R + si-FOXO4 + si-NC group, the activities of oxidative stress indicators SOD and GSH-Px were decreased in the OGD/R + si-FOXO4 + si-CTRP6 group, while ROS levels increased (Fig. 7D). Moreover, decreased levels of inflammatory cytokines IL-6, IL-1β and TNF-a in the OGD/R + si-FOXO4 + si-NC group were significantly increased in the OGD/R + si-FOXO4 + si-CTRP6 group (Fig. 7E).

Knockdown of FOXO4 regulates CTRP6 expression to protect against OGD/R-induced HCMEC/D3 cell injury via the AMPK/Nrf2/heme oxygenase-1 (HO-1) pathway. Expression of AMPK/Nrf2/HO-1 pathway-associated proteins phosphorylated (p-)AMPK, Nrf2 and HO-1 were significantly decreased following OGD/R induction. After interfering with the expression of FOXO4, expression of p-AMPK, Nrf2 and HO-1 in OGD/R-induced HCMEC/D3 cells was increased. Compared with the OGD/R + si-FOXO4 + si-NC group, the expression of p-AMPK, Nrf2 and HO-1

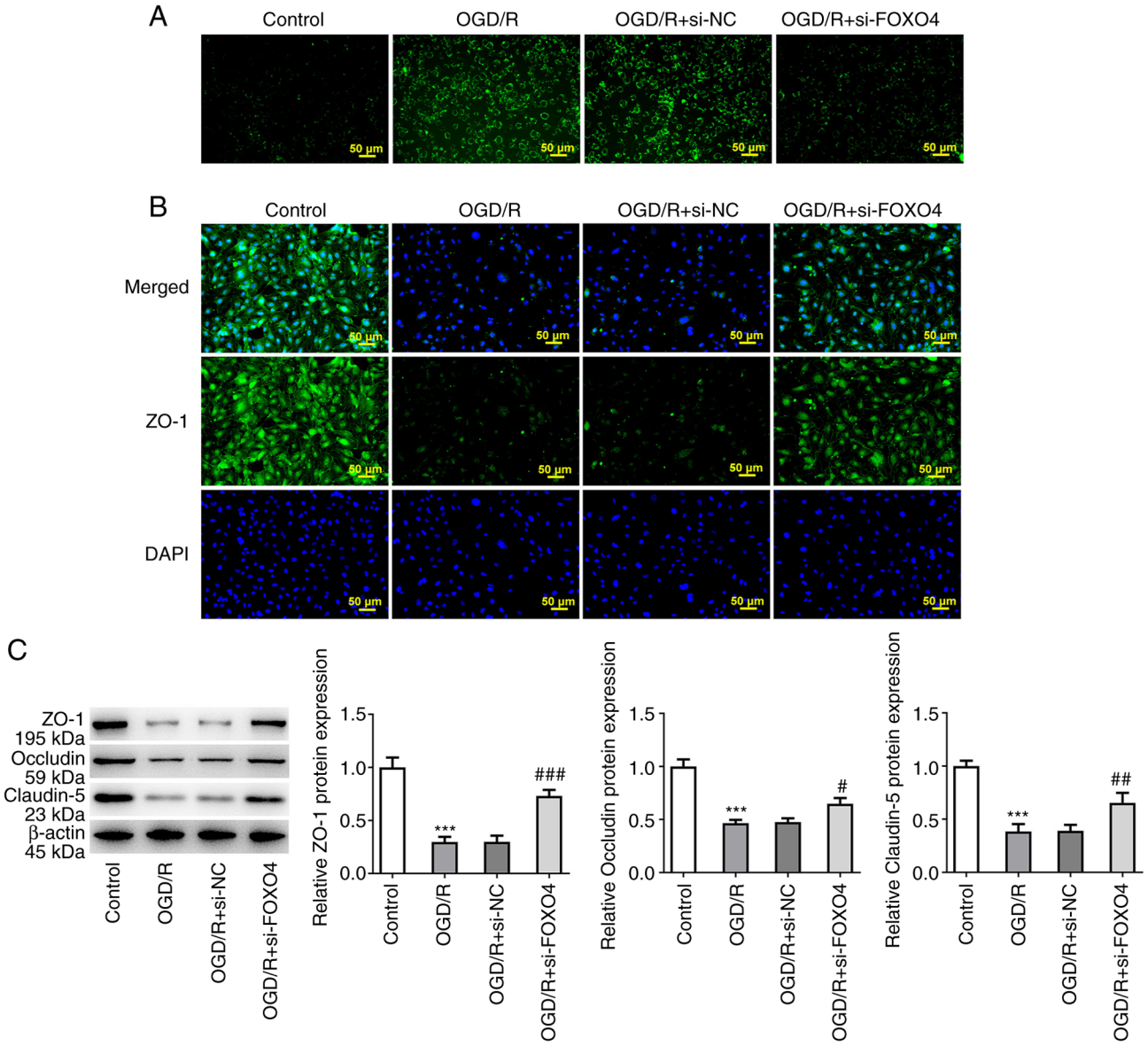

Figure 3. Knockdown of FOXO4 improves OGD/R-induced HCMEC/D3 cell barrier dysfunction. (A) FITC-Dextran kit was used to detect endothelial permeability. (B) Immunofluorescence detected expression of tight junction protein ZO-1. (C) Western blotting detected the expression of tight junction proteins ZO-1, occludin and claudin-5. ***P<0.001 vs. control; $^{\#}$P<0.05, $^{\#\#}$P<0.01, $^{\#\#\#}$P<0.001 vs. OGD/R + si-NC. OGD/R, oxygen-glucose deprivation/reoxygenation; FOXO4, forkhead box protein O4; NC, negative control; ZO-1, zonula occludens-1; si, small interfering.

in the OGD/R + si-FOXO4 + SI-NC group was significantly decreased (Fig. 8).

Discussion

IS exerts damaging effects on cerebral microcirculation such as oxidative stress, excessive secretion of inflammatory mediators, leukocyte infiltration, increased permeability of microvessels, destruction of the blood-brain barrier (BBB) and calcium overload (13). BMECs, highly specialized endothelial cells, are a core component of the BBB and play an important role in maintaining the function of the BBB, dynamic balance of the cerebral microvascular system and normal cerebral blood flow (14). BMECs are key targets affected by cerebral ischemic injury (15,16). BMECs are sensitive to ischemia and hypoxia (17). Multiple studies have used OGD/R to induce BMEC ischemic injury *in vitro* (18,19). After cerebral ischemic injury, BMECs shed and denature from the vascular wall, leading to release of inflammatory factors TNF-α, IL-1β and IL-6 (20). The permeability of the BBB is increased, and the structural and functional integrity of cells is damaged, resulting in endothelial cell dysfunction and brain parenchymal injury (21). In the present study, following OGD/R induction, cell viability was decreased and apoptosis, inflammatory factor release and oxidative stress levels were increased. Moreover, HCMEC/D3 cell barrier function was impaired following OGD/R induction. These results indicated that a BMEC injury model was successfully constructed.

Previous studies have shown that FOXO4 is highly expressed during IRI in the liver (9), kidney (5) and heart (22). In addition, FOXO4 is expressed in OGD/R-treated human cortical neurons, suggesting that FOXO4 may participate in cerebral stroke (23). To the best of our knowledge, the present study is the first to demonstrate that FOXO4 expression is

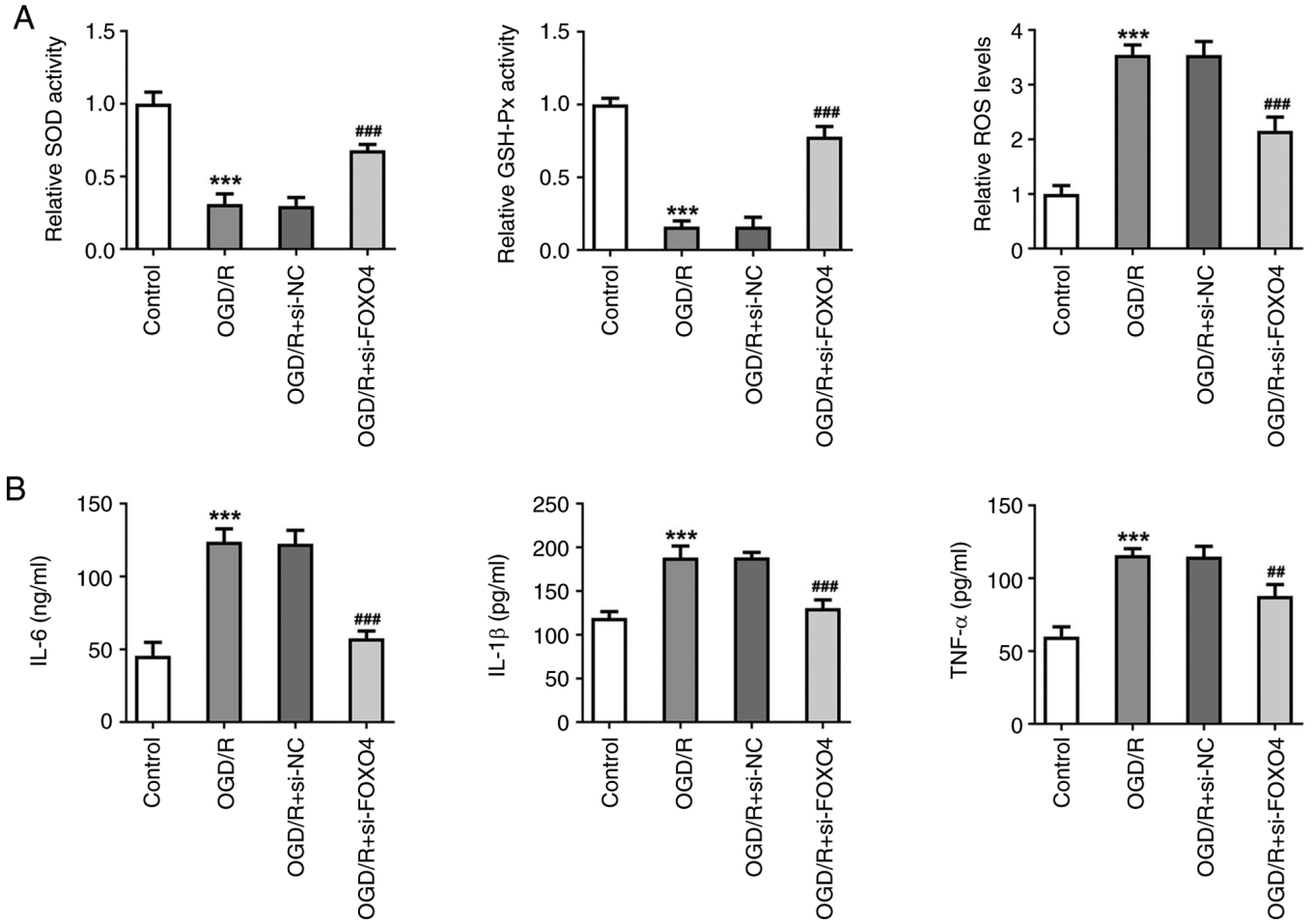

Figure 4. Knockdown of FOXO4 alleviates OGD/R-induced oxidative stress and inflammation in HCMEC/D3 cells. (A) Levels of oxidative stress-associated indicators SOD, GSH-Px and ROS. (B) ELISA was used to detect levels of inflammatory cytokines in cells. ***P<0.001 vs. control; ##P<0.01, ###P<0.001 vs. OGD/R + si-NC. OGD/R, oxygen-glucose deprivation/reoxygenation; FOXO4, forkhead box protein O4; NC, negative control; SOD, superoxide dismutase, GSH-Px, glutathione peroxidase; ROS, reactive oxygen species; si, small interfering.

abnormally elevated in OGD/R-induced HCMEC/D3 cells. Apoptosis is a process of programmed cell death that is involved in the pathogenesis of CIRI (24,25). FOXO4 can contribute to apoptosis during hepatic (9), myocardial (22) and renal IRI (5). In the present study, it was observed that interference with FOXO4 expression significantly inhibited OGD/R-induced HCMEC/D3 cell apoptosis, accompanied by elevated anti-apoptotic Bcl-2 expression and decreased pro-apoptotic Bax and cleaved caspase 3 expression. The destruction of the BBB is a key factor in the occurrence and development of IS (26,27). The BBB is mainly composed of BMECs, tight junction structures, pericytes, astrocytes, foot processes and basement membranes (14). These structures and biological properties enable it to selectively control the exchange of substances between blood and brain tissue, serving a key role in maintaining the homeostasis of the central nervous system environment (14). Tight junction proteins, including ZO-1, claudin-5 and occludin, are key in regulating the integrity and permeability of BBB and are disrupted and redistributed following IS (28). In the present study, FOXO4 silencing promoted ZO-1, claudin-5 and occludin expression, indicating that FOXO4 downregulation improved the barrier dysfunction in OGD/R-exposed HCMEC/D3 cells. Oxidative stress and inflammatory response are common events responsible for CIRI (29). Oxidative stress-activated FOXO proteins (30) regulate the expression of oxidative stress-related genes (31). Moreover, FOXO4 knockdown decreases ROS generation and increases SOD and GSH-Px activities following IRI (10,22). Here, in OGD/R-exposed HCMEC/D3 cells, interference with FOXO4 served a protective role in oxidative stress, demonstrated by improved SOD and GSH-Px activities and decreased ROS levels. Furthermore, downregulation of FOXO4 decreased levels of proinflammatory cytokines including IL-6, IL-1β and TNF-α. These results suggested that interference with FOXO4 expression might inhibit oxidative stress, inflammation and apoptosis in cell damage in CIRI.

FOXO4 is a transcription factor that binds to the promoters of a broad variety of target genes and controls several cellular processes (32). For example, FOXO4 aggravates apoptosis and oxidative stress of H/R-induced cardiomyocytes through negative modulation of USP10 transcription (10). In the present study, the binding sites of transcription factor FOXO4 and CTRP6 promoter were predicted using the HDOCK SERVER database. The binding between FOXO4 and the CTRP6 promoter was further verified by mechanism assays and CTRP6 expression was demonstrated to be depleted

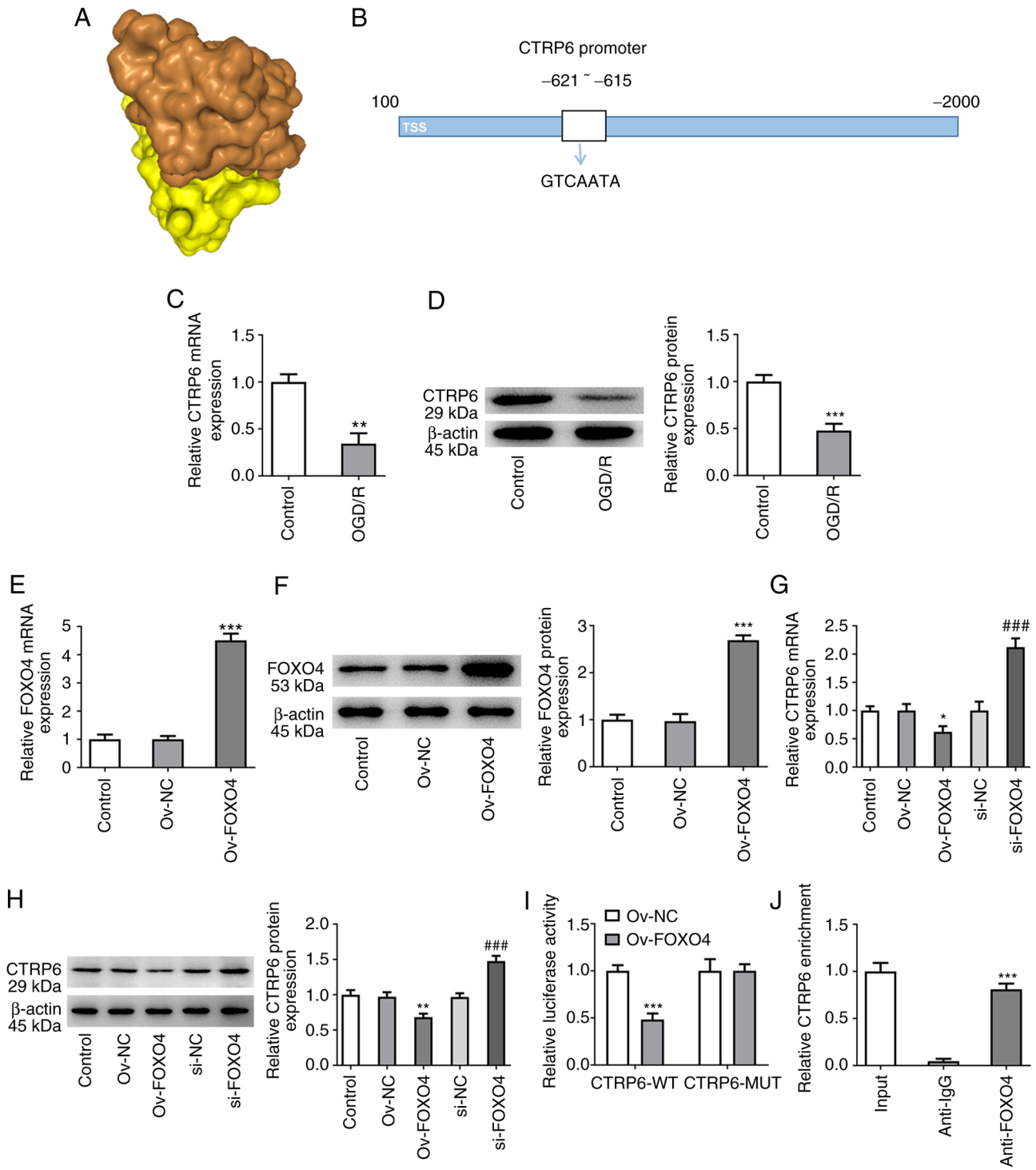

Figure 5. Knockdown of FOXO4 regulates CTRP6 transcription in HCMEC/D3 cells. (A) HDOCK SERVER database predicted the binding of FOXO4 to CTRP6. (B) Potential binding sequences between FOXO4 and CTRP6 promoter were predicted by JASPAR database. Expression of CTRP6 was detected by (C) RT-qPCR and (D) western blotting. **P<0.01, ***P<0.001 vs. control. FOXO4 overexpression plasmid was transfected. (E) RT-qPCR and (F) western blotting detected the cell transfection efficiency. (G) RT-qPCR and (H) western blotting were used to detect the expression of FOXO4. *P<0.05, **P<0.01, ***P<0.001 vs. Ov-NC; $^{\#\#\#}$P<0.001 vs. si-NC. (I) Luciferase detection and (J) ChIP assay demonstrated the binding ability of FOXO4 and CTRP6 promoter. ***P<0.001 vs. Ov-NC. OGD/R, oxygen-glucose deprivation/reoxygenation; FOXO4, forkhead box protein O4; NC, negative control; CTRP6, C1q/tumor necrosis factor-related protein 6; ChIP, chromatin immunoprecipitation; si, small interfering; ov, overexpression; RT-q, reverse transcription-quantitative; WT, wild-type; MUT, mutant; TSS, Transcription start site.

after FOXO4 was overexpressed and to be raised when FOXO4 was down-regulated, suggesting that FOXO4 could transcriptionally inhibit expression of CTRP6. Furthermore, it was hypothesized that knockdown of FOXO4 could upregulate the expression of CTRP6, thereby protecting against OGD/R-induced HCMEC/D3 cell damage. CTRP is a highly conserved family of adiponectin-like proteins involved in a variety of physiological processes, such as cell proliferation, lipid metabolism, insulin sensitivity, energy balance and cardiac protection (33). CTRP6 decreases damage of the central

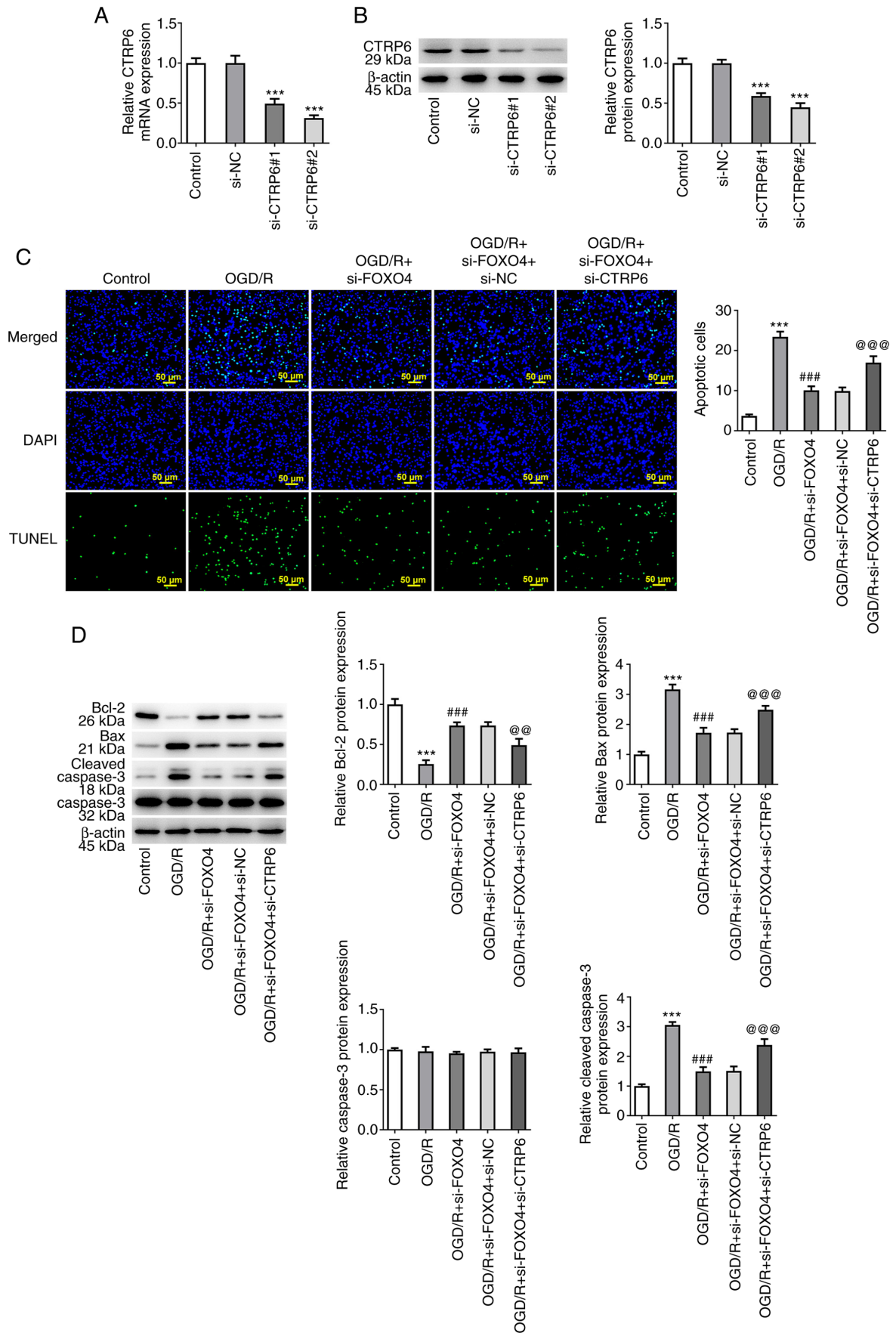

Figure 6. Knockdown of FOXO4 regulates expression of CTRP6 to protect against OGD/R-induced HCMEC/D3 cell damage. CTRP6 interference plasmid was transfected. (A) Reverse transcription-quantitative PCR and (B) western blotting detected transfection efficiency. ***P<0.001 vs. si-NC. (C) Apoptosis was detected by TUNEL assay. (D) Western blotting detected expression of apoptosis-related proteins. ***P<0.001 vs. control; $^{###}$P<0.001 vs. OGD/R; $^{@@}$P<0.01, $^{@@@}$P<0.001 vs OGD/R + si-FOXO4 + si-NC. OGD/R, oxygen-glucose deprivation/reoxygenation; FOXO4, forkhead box protein O4; NC, negative control; CTRP6, C1q/tumor necrosis factor-related protein 6; si, small interfering.

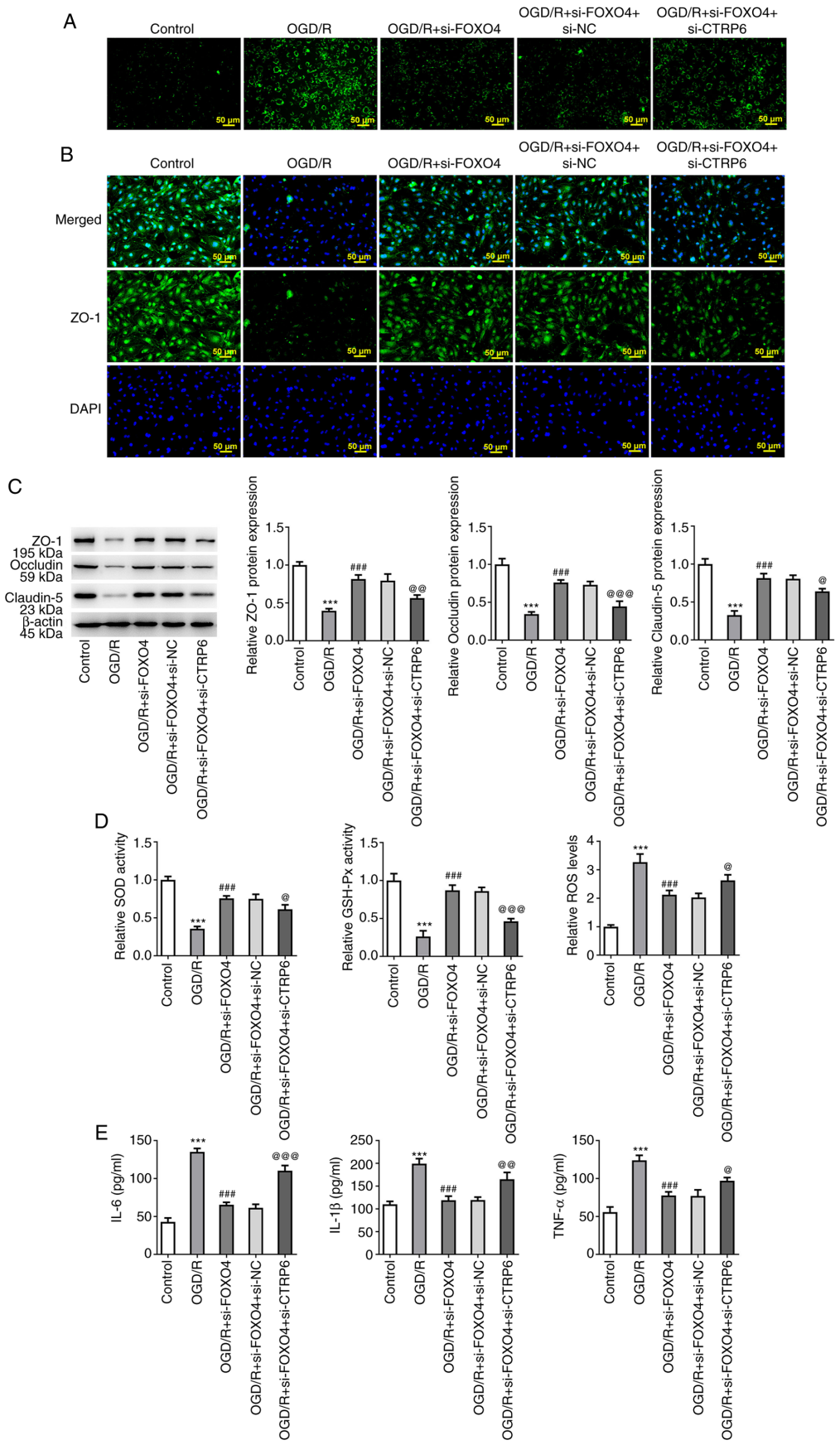

Figure 7. Knockdown of FOXO4 regulates expression of CTRP6 to protect against OGD/R-induced HCMEC/D3 cell damage. (A) FITC-Dextran kit was used to detect endothelial permeability. (B) Immunofluorescence assay detected expression of tight junction protein ZO-1. (C) Western blotting detected expression of tight junction proteins ZO-1, occludin and claudin-5. (D) Levels of oxidative stress-associated indicators SOD, GSH-Px and ROS. (E) ELISA was used to detect levels of inflammatory cytokines in cells. ***P<0.001 vs. control; $^{###}$P<0.001 vs. OGD/R; $^{@}$P<0.05, $^{@@}$P<0.01, $^{@@@}$P<0.001 vs. OGD/R + si-FOXO4 + si-NC. OGD/R, oxygen-glucose deprivation/reoxygenation; FOXO4, forkhead box protein O4; NC, negative control; CTRP6, C1q/tumor necrosis factor-related protein 6; ZO-1, zonula occludens-1; si, small interfering; SOD, superoxide dismutase; GSH-Px, glutathione peroxidase; ROS, reactive oxygen species.

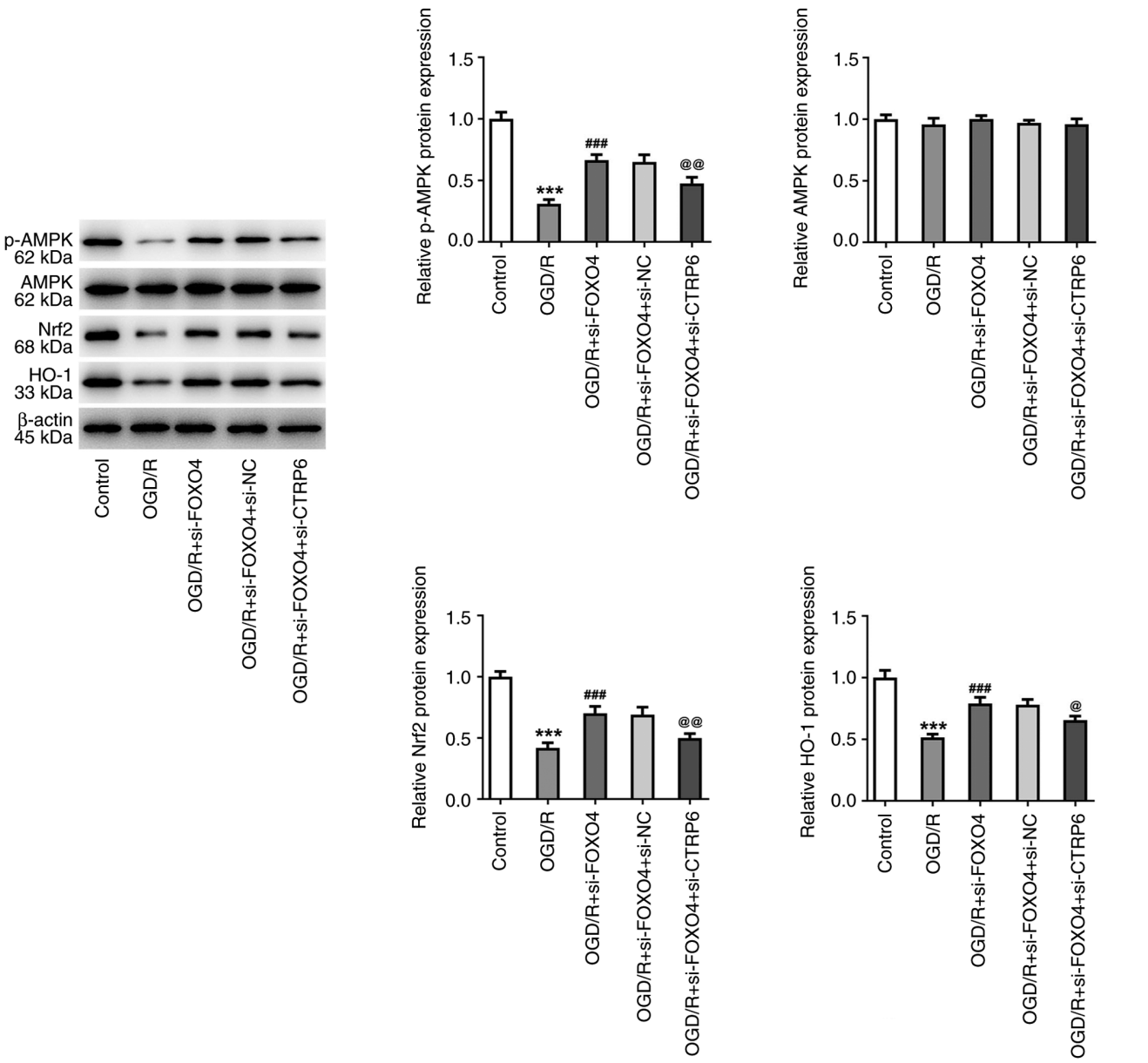

Figure 8. Knockdown of FOXO4 regulates expression of CTRP6 to protect against OGD/R-induced HCMEC/D3 cell damage via the AMPK/Nrf2/HO-1 pathway. Western blotting detected expression of AMPK/Nrf2/HO-1 pathway-associated proteins p-AMPK, Nrf2 and HO-1. ***P<0.001 vs. control; $^{###}$P<0.001 vs. OGD/R; $^{@}$P<0.05, $^{@@}$P<0.01 vs. OGD/R + si-FOXO4 + si-NC. OGD/R, oxygen-glucose deprivation/reoxygenation; FOXO4, forkhead box protein O4; NC, negative control; CTRP6, C1q/tumor necrosis factor-related protein 6; HO-1, heme oxygenase-1; si, small interfering; p-, phosphorylated.

nervous system induced by sevoflurane by promoting expression of p-Akt (34). CTRP6 protects against CIRI by reducing inflammation, oxidative stress and apoptosis of rat pheochromocytoma (PC12) cells (35). CTRP6 improves peroxisome proliferator-activated receptor γ activation to relieve vascular endothelial dysfunction in angiotensin II-induced hypertension and spontaneously hypertensive rats (36). These results indicate that CTRP6 serves an important role in the occurrence and development of cerebral ischemia. In the present study, inhibition of CTRP6 partially reversed the suppressive effect of FOXO4 knockdown on apoptosis, BBB dysfunction and oxidative stress in OGD/R-exposed HCMEC/D3 cells.

The downstream pathway of CTRP6 was investigated. CTRP6 regulates microRNA-34a-5p expression via the AMPK/sirtuin 1 pathway to inhibit TNF-α-induced apoptosis of salivary gland cells (37). In renal fibrosis, CTRP6 inhibits extracellular matrix deposition and promotes AMPK phosphorylation by promoting fatty acid oxidation (38). Palmatine prevents CIRI by activating the AMPK/Nrf2 pathway (39). Salvinorin A alleviates BBB and brain microvascular endothelial cell injury following IRI and alleviates endoplasmic reticulum stress of endothelial cells via the AMPK pathway (40). MitoQ protects against BMEC damage induced by high glucose levels via the Nrf2/HO-1 pathway (41). Therefore, it was hypothesized that FOXO4 could regulate CTRP6 and downstream AMPK/Nrf2/HO-1 signaling, thus serving a role in OGD/R-induced BMEC injury. In the present study, FOXO4 depletion regulated expression of CTRP6, thereby modulating the AMPK/Nrf2/HO-1 signaling pathway. However, inhibitors or activators of the AMPK/Nrf2/HO-1 pathway were not used

to explore the mechanism, which is a limitation of the present study and requires further exploration in future experiments. Furthermore, middle cerebral artery occlusion is the most widely used IS model (42). Hence, animal experiments should be performed to focus on the effects of FOXO4 and CTRP6 on CIRI using middle cerebral artery occlusion models to corroborate the findings of the present study. Moreover, the specific role of FOXO4 and CTRP6 in the infarction area in the brain needs to be investigated in *in vivo* models.

Overall, FOXO4 knockdown activated expression of CTRP6 to protect against cerebral microvascular endothelial cell injury induced by OGD/R via the AMPK/Nrf2/HO-1 pathway. The present study suggested that FOXO4 and CTRP6 might serve as promising biomarkers for IS.

Acknowledgements

Not applicable.

Funding

No funding was received.

Availability of data and materials

All data generated or analyzed during this study are included in this published article.

Authors' contributions

XC, ZL and YY designed the study and wrote and revised the manuscript. XC and YY analyzed the data and performed the literature review. All authors performed the experiments. XC and YY confirm the authenticity of all the raw data. All authors have read and approved the final manuscript.

Ethics approval and consent to participate

Not applicable.

Patient consent for publication

Not applicable.

Competing interests

The authors declare that they have no competing interests.

References

1. GBD 2019 Stroke Collaborators: Global, regional, and national burden of stroke and its risk factors, 1990-2019: A systematic analysis for the global burden of disease study 2019. Lancet Neurol 20: 795-820, 2021.
2. Gittler M and Davis AM: Guidelines for adult stroke rehabilitation and recovery. JAMA 319: 820-821, 2018.
3. Derex L and Cho TH: Mechanical thrombectomy in acute ischemic stroke. Rev Neurol (Paris) 173: 106-113, 2017.
4. Kapanova G, Tashenova G, Akhenbekova A, Tokpınar A and Yılmaz S: Cerebral ischemia reperfusion injury: From public health perspectives to mechanisms. Folia Neuropathol 60: 384-389, 2022.
5. Liu H, Wang L, Weng X, Chen H, Du Y, Diao C, Chen Z and Liu X: Inhibition of Brd4 alleviates renal ischemia/reperfusion injury-induced apoptosis and endoplasmic reticulum stress by blocking FoxO4-mediated oxidative stress. Redox Biol 24: 101195, 2019.
6. Liu W, Li Y and Luo B: Current perspective on the regulation of FOXO4 and its role in disease progression. Cell Mol Life Sci 77: 651-663, 2020.
7. Orea-Soufi A, Paik J, Bragança J, Donlon TA, Willcox BJ and Link W: FOXO transcription factors as therapeutic targets in human diseases. Trends Pharmacol Sci 43: 1070-1084, 2022.
8. Liu XL, Gao CC, Qi M, Han YL, Zhou ML and Zheng LR: Expression of FOXO transcription factors in the brain following traumatic brain injury. Neurosci Lett 753: 135882, 2021.
9. He B, Yang F, Ning Y and Li Y: Sevoflurane alleviates hepatic ischaemia/reperfusion injury by up-regulating miR-96 and down-regulating FOXO4. J Cell Mol Med 25: 5899-5911, 2021 (Epub ahead of print).
10. Huang J, Liu Y, Wang M, Wang R, Ling H and Yang Y: FoxO4 negatively modulates USP10 transcription to aggravate the apoptosis and oxidative stress of hypoxia/reoxygenation-induced cardiomyocytes by regulating the Hippo/YAP pathway. J Bioenerg Biomembr 53: 541-551, 2021.
11. Yan Y, Tao H, He J and Huang SY: The HDOCK server for integrated protein-protein docking. Nat Protoc 15: 1829-1852, 2020.
12. Livak KJ and Schmittgen TD: Analysis of relative gene expression data using real-time quantitative PCR and the 2(-Delta Delta C(T)) method. Methods 25: 402-408, 2001.
13. Zhu H, Wang Z, Xing Y, Gao Y, Ma T, Lou L, Lou J, Gao Y, Wang S and Wang Y: Baicalin reduces the permeability of the blood-brain barrier during hypoxia in vitro by increasing the expression of tight junction proteins in brain microvascular endothelial cells. J Ethnopharmacol 141: 714-720, 2012.
14. Ferro MP, Heilshorn SC and Owens RM: Materials for blood brain barrier modeling in vitro. Mater Sci Eng R Rep 140: 100522, 2022.
15. del Zoppo GJ and Hallenbeck JM: Advances in the vascular pathophysiology of ischemic stroke. Thromb Res 98: 73-81, 2000.
16. Ishikawa M, Zhang JH, Nanda A and Granger DN: Inflammatory responses to ischemia and reperfusion in the cerebral microcirculation. Front Biosci 9: 1339-1347, 2004.
17. Engelhardt S, Huang SF, Patkar S, Gassmann M and Ogunshola OO: Differential responses of blood-brain barrier associated cells to hypoxia and ischemia: A comparative study. Fluids Barriers CNS 12: 4, 2015.
18. Fan XD, Yao MJ, Yang B, Han X, Zhang YH, Wang GR, Li P, Xu L and Liu JX: Chinese herbal preparation sailuotong alleviates brain ischemia via Nrf2 antioxidation pathway-dependent cerebral microvascular protection. Front Pharmacol 12: 748568, 2021.
19. Jiang W, Li J, Cai Y, Liu W, Chen M, Xu X, Deng M, Sun J, Zhou L, Huang Y, *et al*: The novel lncRNA ENST00000530525 affects ANO1, contributing to blood-brain barrier injury in cultured hCMEC/D3 cells under OGD/R conditions. Front Genet 13: 873230, 2022.
20. Li F, Li W, Li X, Li F, Zhang L, Wang B, Huang G, Guo X, Wan L, Liu Y, *et al*: Geniposide attenuates inflammatory response by suppressing P2Y14 receptor and downstream ERK1/2 signaling pathway in oxygen and glucose deprivation-induced brain microvascular endothelial cells. J Ethnopharmacol 185: 77-86, 2016.
21. Lin Q, Wang W, Yang L and Duan X: 4-Methoxybenzylalcohol protects brain microvascular endothelial cells against oxygen-glucose deprivation/reperfusion-induced injury via activation of the PI3K/AKT signaling pathway. Exp Ther Med 21: 252, 2021.
22. Yu L, Zhang W, Huang C, Liang Q, Bao H, Gong Z, Xu M, Wang Z, Wen M and Cheng X: FoxO4 promotes myocardial ischemia-reperfusion injury: The role of oxidative stress-induced apoptosis. Am J Transl Res 10: 2890-2900, 2018.
23. Yan B, Jin Y, Mao S, Zhang Y, Yang D, Du M and Yin Y: Smurf2-mediated ubiquitination of FOXO4 regulates oxygen-glucose deprivation/reperfusion-induced pyroptosis of cortical neurons. Curr Neurovasc Res: Oct 12, 2023 (Epub ahead of print).
24. Li K, Ding D and Zhang M: Neuroprotection of osthole against cerebral ischemia/reperfusion injury through an anti-apoptotic pathway in rats. Biol Pharm Bull 39: 336-342, 2016.
25. Wu T, Yin F, Kong H and Peng J: Germacrone attenuates cerebral ischemia/reperfusion injury in rats via antioxidative and anti-apoptotic mechanisms. J Cell Biochem 120: 18901-18909, 2019.

26. Shah K and Abbruscato T: The role of blood-brain barrier transporters in pathophysiology and pharmacotherapy of stroke. Curr Pharm Des 20: 1510-1522, 2014.
27. Yin KJ, Hamblin M and Chen YE: Non-coding RNAs in cerebral endothelial pathophysiology: Emerging roles in stroke. Neurochem Int 77: 9-16, 2014.
28. Abdullahi W, Tripathi D and Ronaldson PT: Blood-brain barrier dysfunction in ischemic stroke: Targeting tight junctions and transporters for vascular protection. Am J Physiol Cell Physiol 315: C343-C356, 2018.
29. Li M, Tang H, Li Z and Tang W: Emerging treatment strategies for cerebral ischemia-reperfusion injury. Neuroscience 507: 112-124, 2022.
30. Brunet A, Bonni A, Zigmond MJ, Lin MZ, Juo P, Hu LS, Anderson MJ, Arden KC, Blenis J and Greenberg ME: Akt promotes cell survival by phosphorylating and inhibiting a Forkhead transcription factor. Cell 96: 857-868, 1999.
31. Storz P: Forkhead homeobox type O transcription factors in the responses to oxidative stress. Antioxid Redox Signal 14: 593-605, 2011.
32. Link W: Introduction to FOXO biology. Methods Mol Biol 1890: 1-9, 2019.
33. Dong X, Hu H, Fang Z, Cui J and Liu F: CTRP6 inhibits PDGF-BB-induced vascular smooth muscle cell proliferation and migration. Biomed Pharmacother 103: 844-850, 2018.
34. Liu Z and Yang B: CTRP6[C1q/tumor necrosis factor (TNF)-related protein-6] alleviated the sevoflurane induced injury of mice central nervous system by promoting the expression of p-Akt (phosphorylated Akt). Bioengineered 12: 5716-5726, 2021.
35. Li Y, Sun J, Gu L and Gao X: Protective effect of CTRP6 on cerebral ischemia/reperfusion injury by attenuating inflammation, oxidative stress and apoptosis in PC12 cells. Mol Med Rep 22: 344-352, 2020.
36. Chi L, Hu X, Zhang W, Bai T, Zhang L, Zeng H, Guo R, Zhang Y and Tian H: Adipokine CTRP6 improves PPARγ activation to alleviate angiotensin II-induced hypertension and vascular endothelial dysfunction in spontaneously hypertensive rats. Biochem Biophys Res Commun 482: 727-734, 2017.
37. Qu LH, Hong X, Zhang Y, Cong X, Xiang RL, Mei M, Su JZ, Wu LL and Yu GY: C1q/tumor necrosis factor-related protein-6 attenuates TNF-α-induced apoptosis in salivary acinar cells via AMPK/SIRT1-modulated miR-34a-5p expression. J Cell Physiol 236: 5785-5800, 2021.
38. Xie YH, Xiao Y, Huang Q, Hu XF, Gong ZC and Du J: Role of the CTRP6/AMPK pathway in kidney fibrosis through the promotion of fatty acid oxidation. Eur J Pharmacol 892: 173755, 2021.
39. Tang C, Hong J, Hu C, Huang C, Gao J, Huang J, Wang D, Geng Q and Dong Y: Palmatine protects against cerebral ischemia/reperfusion injury by activation of the AMPK/Nrf2 pathway. Oxid Med Cell Longev 2021: 6660193, 2021.
40. Xin J, Ma X, Chen W, Zhou W, Dong H, Wang Z and Ji F: Regulation of blood-brain barrier permeability by Salvinorin A via alleviating endoplasmic reticulum stress in brain endothelial cell after ischemia stroke. Neurochem Int 149: 105093, 2021.
41. Yang MY, Fan Z, Zhang Z and Fan J: MitoQ protects against high glucose-induced brain microvascular endothelial cells injury via the Nrf2/HO-1 pathway. J Pharmacol Sci 145: 105-114, 2021.
42. Chaparro-Cabanillas N, Arbaizar-Rovirosa M, Salas-Perdomo A, Gallizioli M, Planas AM and Justicia C: Transient middle cerebral artery occlusion model of stroke. J Vis Exp: Aug 11, 2023 (Epub ahead of print). doi: 10.3791/65857. 2023.